Original Research

Improved Blood Suppression in Three-Dimensional (3D) Fast Spin-Echo (FSE) Vessel Wall Imaging Using a Combination of Double Inversion-Recovery (DIR) and Diffusion Sensitizing Gradient (DSG) Preparations

Mahender K. Makhijani, MS,[*] Houchun H. Hu, PhD, Gerry M. Pohost, MD, and Krishna S. Nayak, PhD

Purpose: To provide improved blood suppression in three-dimensional inner-volume fast spin-echo (3D IV-FSE) carotid vessel wall imaging by using a hybrid preparation consisting of double inversion-recovery (DIR) and diffusion sensitizing gradients (DSG).

Materials and Methods: Multicontrast black-blood MRI is widely used for vessel wall imaging and characterization of atherosclerotic plaque composition. Blood suppression is difficult when using 3D volumetric imaging techniques. DIR approaches do not provide robust blood suppression due to incomplete replacement of blood spins, and DSG approaches compromise vessel wall signal, reducing the lumen-wall contrast-to-noise ratio efficiency (CNR_{eff}). In this work a hybrid DIR+DSG preparation is developed and optimized for blood suppression, vessel wall signal preservation, and vessel-wall contrast in 3D IV-FSE imaging. Cardiac gated T_1-weighted carotid vessel wall images were acquired in five volunteers with $0.5 \times 0.5 \times 2.5$ mm^3 spatial resolution in 80 seconds.

Results: Data from healthy volunteers indicate that the proposed method yields a statistically significant ($P < 0.01$) improvement in blood suppression and lumen-wall CNR_{eff} compared to standard DIR and standard DSG methods alone.

Conclusion: A combination of DIR and DSG preparations can provide improved blood suppression and lumen-wall CNR_{eff} for 3D IV-FSE vessel wall imaging.

ATHEROSCLEROSIS AFFECTS MORE THAN 18 MILLION AMERICANS. The fundamental processes leading to myocardial infarction and thrombotic stroke are the formation, growth, and rupture of intraarterial atherosclerotic plaque. Atherosclerotic disease of the carotid arteries is estimated to cause 40% of stroke producing thrombi. High-resolution MRI has been shown to identify atherosclerotic carotid plaque (1–3), and optimized multispectral pulse sequences have been developed for vessel wall delineation and plaque characterization (4). In several of these sequences, a preparatory sequence is used for blood suppression in order to improve vessel wall contrast with respect to the lumen, and is followed by rapid imaging sequences that are capable of differentiating the various potential plaque components.

Two-dimensional (2D) multislice fast spin-echo (FSE) with double inversion-recovery (DIR) preparation (4) is the most widely used pulse sequence for this application. Four image sets (proton-density-, T_1-, T_2-weighted FSE and time of flight (4)) are typically acquired across a 2- to 3-cm segment around the bifurcation. The main limitations of these 2D methods are low signal-to-noise ratio (SNR), lack of contiguous anatomic coverage, quantitation errors due to partial volume effects, and long scan times. Multiple averages are required even at 3T (5,6), in order to achieve clinically useful SNR and spatial resolution. This results in long scan times on the order of 5 to 7 minutes per slice for all three forms of FSE-based contrast (4–6). Scan time reduction can be achieved by interleaving multiple slices (7–12) but

at the cost of possible artifacts from incomplete blood suppression due to imperfect T_1-nulling in all but one of the slices.

Crowe et al (13) utilized 3D inner volume (IV) (14,15) acquisitions to alleviate the inherent SNR limitations of 2D methods along with DIR preparation for blood suppression. IV-FSE is a variant of standard FSE in which the excitation and refocusing pulses are applied on orthogonal spatial axes. This enables significant scan time reduction, since the excited field of view (FOV) is reduced in one of the phase-encoding directions, allowing for lesser number of phase encoding steps. DIR preparation inverts all blood spins outside of the imaging volume while static spins within the acquisition volume are realigned with the equilibrium state. The acquisition window is delayed from DIR preparation to coincide with null point of blood T_1, thus giving the effect of blood suppression. The efficacy of DIR preparation depends on the outflow of unaffected blood spins within the imaging volume. In some subjects, blood spins do not completely wash out of the imaging volume by the time of data acquisition resulting in residual blood signal. Hence, directly applying DIR preparation to 3D carotid imaging can lead to artifacts from unsuppressed blood signal (16) near the bifurcation. Such artifacts may mimic the presence of plaque (17) and/or lead to inaccurate vessel wall thickness measurements.

T_1-independent blood suppression techniques have been explored recently. One technique, called diffusion sensitizing gradients (DSG, also known as DPDE, DW-prep, and MSDE), utilizes three or more RF pulses: $90_x – (180_y)^n – 90_{-x}$ with symmetric flow sensitizing gradients pairs on all three axes. Flowing blood spins are suppressed due to phase dispersion induced by the gradients (18). Carotid blood suppression using DSG preparation was first demonstrated by Koktzoglou and Li (19) with 3D steady-state free-precession (SSFP) acquisitions, and later by Wang et al (20) with 2D multislice FSE acquisitions. The main design parameter for this preparation is the amount of sensitization (gradient duration, amplitude, and direction). The gradients should ideally be applied at the maximum hardware limits for the shortest duration that causes sufficient intravoxel dephasing of flowing spins. Applying gradients at peak strength can introduce eddy current–related artifacts. This can be avoided by derating the gradient amplitude but at the cost of further increasing the DSG duration. This eventually leads to loss of critical vessel wall signal due to T_2 decay and true diffusion effects.

In this work we utilize 3D IV-FSE sequence for imaging and hybrid DIR+DSG preparation for blood suppression. The simultaneous application of DIR and DSG preparation has potential advantages when compared to DSG alone or DIR alone. The hybrid DIR+DSG preparation reduces the duration of the DSG component to 11.0 msec from 18.2 msec that is required for the standalone DSG preparation. Hence this hybrid preparation reduces T_2-related signal loss in the vessel wall, which potentially improves vessel wall SNR. The hybrid preparation provides improved blood suppression compared to DIR preparation alone. We demonstrate this hybrid preparation with 3D IV-FSE imaging that captures a 2-cm slab across the carotid bifurcation with $0.5 \times 0.5 \times 2.5$ mm^3 resolution in a single 80-second acquisition, with blood-lumen contrast-to-noise ratio (CNR) > 20 throughout the bifurcation.

MATERIALS AND METHODS
Experimental Setup

Experiments were performed on two commercial 3T systems (one Signa HD and one Signa HDx; GE Healthcare, Waukesha, WI, USA), with gradients capable of 40 mT/m amplitude and 150 T/m/second slew rate, and a receiver capable of 4-μsec sampling. The body coil was used for radio frequency (RF) transmission. A four-channel bilateral carotid array coil (Pathway MRI, Seattle, WA, USA) was used for signal reception in the HD system. A six-channel bilateral carotid array coil (Neo-Coil, Waukesha, WI, USA) was used for signal reception in the HDx system. Volunteers were asked to avoid swallowing during the scan, and scans were repeated if they were unable to do so. The study population consisted of five healthy volunteers. Informed consent was obtained prior to scanning. The study was performed with approval and in compliance with the guidelines set forth by our local Institutional Review Board.

The proposed pulse sequence consists of three modules shown in Fig. 1: DIR preparation and DSG preparation (both for blood suppression), and 3D IV-FSE (for image acquisition).

Blood Suppression: DIR Preparation

DIR preparation consists of two inversion pulses followed by a crusher gradient. One nonselective hard inversion pulse (1.0 msec) is followed by one selective adiabatic inversion pulse (8.6 msec) that restores the magnetization within the imaging volume. Imaging takes place at the null point of blood T_1, given by the inversion time below, adapted from Ref. 21.

$$TI = -T_1 \log((1 + e^{-TR/T_1})/2) \qquad [1]$$

The IR time was computed based on the subject's heart rate at the start of the scan using Eq. [1], and assuming inversion time (TI) = 1550 msec (22). The thickness of the selective inversion is made 1.5 times larger than the imaging slab (23).

Blood Suppression: DSG Preparation

The DSG block shown in Fig. 1 is similar in structure to a T_2-preparation module (24) and consists of three hard pulses: $90_x – 180_y –90_{-x}$ followed by spoiler gradients. The first pulse (duration = 0.5 msec, amplitude = 12 μT, where G = 1000 amperes/m) tips all the spins into the transverse plane, the second pulse (duration 1.0 msec, amplitude 12 μT) refocuses the magnetization, and the third tip-up pulse (duration 0.5 msec, amplitude 12 μT) realigns the spins along the equilibrium direction. The refocusing pulse is sandwiched by a symmetric pair of sensitizing
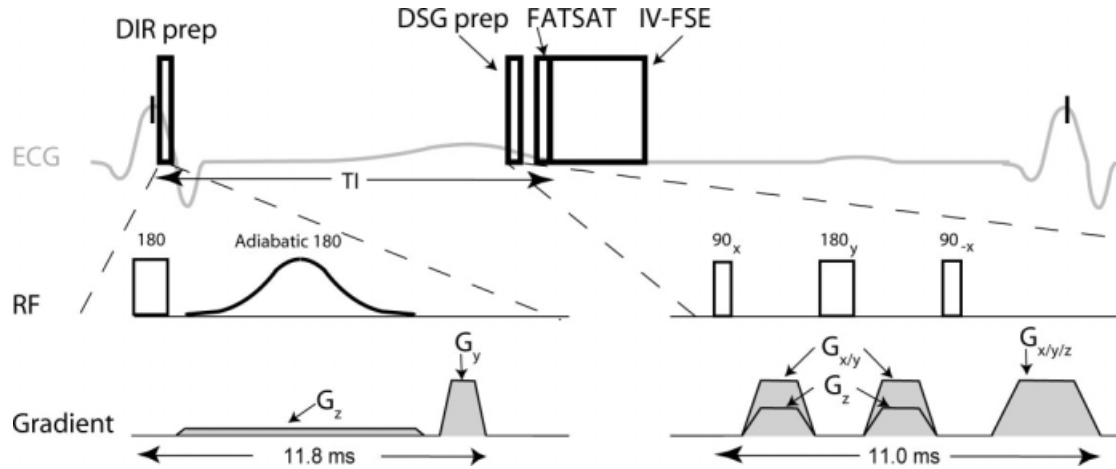
Figure 1. Timing of the proposed pulse sequence. Imaging is performed using a 3D fat-saturated inner-volume fast spin-echo (IV-FSE) pulse sequence. Blood suppression is achieved by a combination of double inversion recovery (DIR) and diffusion sensitizing gradient (DSG) preparations. FATSAT = fat saturation.

gradients that are applied along a combination of the three axes for a duration of 5.2 msec. The gradients and RF pulses are separated by a period of 0.4 msec in order to mitigate eddy current effects. The DSG gradients along the imaging slab (anterior/posterior [A/P] and right/left [R/L]) are set to 40 mT/m while the DSG gradient orthogonal to the imaging slab (superior/inferior [S/I]) is set to 20 mT/m. These amplitudes were determined from phase contrast (PC) velocity measurements discussed later. The total duration of DSG block without the spoiler gradients was 8.8 msec (i.e., the amount of T_2 weighting).

Imaging: 3D IV-FSE

Imaging is preceded by a fat-saturation (FATSAT) sequence, which consists of spectrally selective excitation followed by a crusher gradient. FATSAT improves vessel wall delineation by suppressing perivascular fat (23). The imaging sequence is a variant of FSE, with excitation and all refocusing pulses applied on orthogonal axes. The initial 90° excitation pulse is selective in the A/P direction while the subsequent refocusing pulses are selective in the S/I direction. The refocusing pulses were delivered at a flip angle of 150° due to specific absorption rate (SAR) constraints. Each refocusing pulse is sandwiched by a pair of symmetric crusher gradients to eliminate newly-excited signal due to imperfect refocusing and signal from outside the volume of interest. The excitation pulse is applied along the phase encoding axis while the refocusing pulse is applied along the slab selection axis to minimize echo spacing and maximize readout duty cycle. For the imaging parameters used in this study, the echo spacing would have increased by 0.5 msec if the orientation had been swapped (excitation along the slab direction (S/I), and refocusing along the phase encoding direction (A/P))

A centric phase encoding order was chosen to mitigate ghosting artifacts arising due to phase errors induced by sensitivity to eddy current. Sequential ordering was used in the slice encoding direction. An echo spacing of 6.1 msec was used on the HD system while an echo spacing of 10.2 msec was using on the HDx system. Cardiac-gated T_1-weighted data sets were acquired with scan parameters: TR = 1 RR, echo-train length (ETL) = 10, resolution = $0.5 \times 0.5 \times 2.5$ mm^3, acquired FOV for 2D acquisitions = 16×16 cm^2, and acquired FOV for 3D acquisitions = $16 \times 3.2 \times 2$ cm^3.

Attempted Optimization of DSG Preparation

In five healthy volunteers, we measured the contrast between the vessel wall and luminal blood as a function of the b-value and orientation of the diffusion vector. This procedure involved two experiments. First, the appropriate orientation of the diffusion vector was determined from phase contrast–derived luminal blood velocity measurements. Second, the contrast between vessel wall and lumen was directly measured for several b-values.

The goal of the first experiment was to determine the optimal orientation of diffusion sensitizing gradients in DIR+DSG preparation. For this purpose two datasets were acquired, one with information about the carotid anatomy and the other with luminal blood velocity measurements. Images of the carotid anatomy at the bifurcation were acquired using 3D IV-FSE with the proposed DIR+DSG preparation with diffusion-sensitizing gradients turned off. These images were used to identify locations that suffer from residual luminal blood signal. Luminal blood signal is attenuated due to various aspects of the proposed DIR+DSG preparation including: intravoxel dephasing caused by the diffusion sensitizing bipolar gradient, T_2 weighting caused by the nonzero duration of the preparation, and other system imperfections such as sensitivity to eddy current. In order to isolate the effect of just the bipolar gradient, the anatomical images were acquired using the proposed preparation with only the diffusion-sensitizing bipolar gradient turned off.

Time-resolved velocity maps were obtained using a 3D PC sequence with a resolution of $1.0 \times 1.0 \times 2.5$ mm^3. The anatomic images and velocity maps were
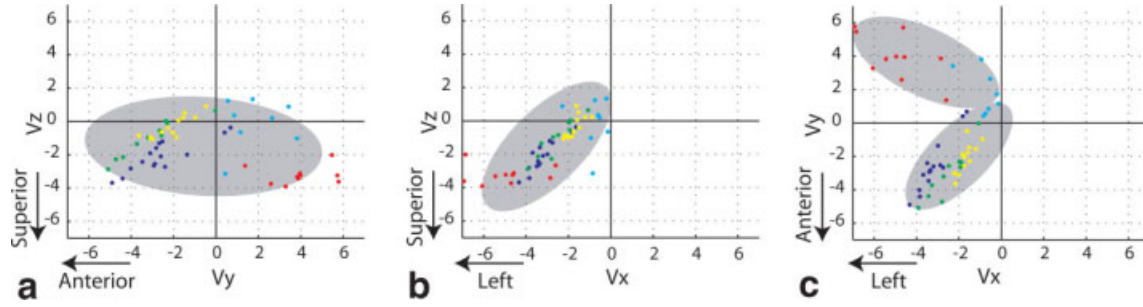
Figure 2. Scatter plots of the velocity (cm/second) of unsuppressed luminal blood. Each color represents one volunteer. **a:** Projection onto the YZ plane, with $(\bar{V}_y, \bar{V}_z)$. = (–0.8, –1.4) and $(\sigma_{Vy}, \sigma_{Vz})$ = (2.96, 1.41). **b:** Projection onto the XZ plane, with $(\bar{V}_x, \bar{V}_z)$. = (–2.7, –1.4) and $(\sigma_{Vx}, \sigma_{Vz})$ = (1.51, 1.41). **c:** Projection onto the XY plane, $(\bar{V}_x, \bar{V}_y)$. = ([–2.3, –2.2], [–3.9, 3.6]) and $(\sigma_{Vx}, \sigma_{Vy})$ = (1.04, 1.64), (2.09, 1.34). Maximum likelihood was used to estimate the mean and standard deviation of one or two component Gaussian mixture distributions for each plot (gray ellipses). Note that $\sigma_{Vy} > \sigma_{Vz}$ but $\sigma_{Vx} \sim \sigma_{Vz}$, hence stronger dephasing is required along the imaging slab (XY or L/R-A/P) rather than perpendicular to the imaging slab (Z or S/I).

registered to obtain velocity vector profiles of the residual luminal blood. These velocity profiles were then used to determine the ratio of in-plane and through-plane velocity components of the unsuppressed blood. This ratio is indicative of the directional preference of the residual blood and was used to determine the relative amplitudes of the sensitizing gradients parallel and orthogonal to the imaging slab.

After the relative strengths of all three sensitizing gradients were established, we performed an experiment to determine the most appropriate gradient area and duration (hence *b*-value). DIR+DSG prepared carotid vessel wall image sets were acquired with various *b*-values. The vessel wall and lumen regions of interest (ROIs) were manually segmented and the corresponding SNR in the ROI for each acquired image was measured. Vessel wall and lumen SNR was plotted as a function of *b*-value and an acceptable tradeoff was determined.

Comparison of Blood Suppression Techniques

T_1-weighted axial datasets were acquired with 3D IV-FSE DIR+DSG, 3D IV-FSE DIR, and conventional 2D multislice FSE DIR scans in five healthy volunteers across the carotid bifurcation. This was done to facilitate a fair comparison and evaluate blood suppression levels using the proposed technique. All the relevant scan parameters, including in-plane spatial resolution, FOV, and slice thickness, were identical for all three methods. For the 3D methods the DIR slab thickness was set to 3 cm, while for the 2D methods it was set to 7.5 mm. The IR time was computed based on the subject's heart rate at the start of the scan using Eq. [1], and assuming T_1 = 1550 msec (22). For example, TI = 350 msec for a heart rate of 75 beats per minute (bpm).

Image Analysis

SNR measurements were based on manually drawn ROIs from the vessel wall and lumen. Noise standard deviation (σ_n) was measured by choosing a represen-

tative ROI in the air space that did not contain any structure. SNR was computed for the vessel wall (SNR_W) and lumen (SNR_L) from the magnitude images by using the relation $0.695S/\sigma_n$, where S represents the average signal intensity in the aforementioned ROIs. CNR was computed by the relation $0.695(S_W - S_L)/\sigma_n$ from the magnitude images. CNR efficiency (CNR_{eff}) was calculated using the relation $CNR_{eff} = CNR/\sqrt{T_{scan}}$, where T_{scan} represents the per slice acquisition time in minutes (17). A two-tailed paired *t*-test was used to determine the statistical significance of the difference in vessel wall SNR, lumen SNR, and wall-to-lumen CNR_{eff} measured using the various techniques. Statistical significance was defined at $P < 0.01$, in all tests.

RESULTS

Attempted Optimization of DSG Preparation

Figure 2 contains scatter-plots representing the velocities of residual luminal blood from five volunteers. The spread of the velocity component along the A/P (Y-axis) was greater than the spread of the through-plane velocity component in every volunteer by 40% to 100%. The amplitude ratio of in-plane to through-plane sensitizing gradients in the proposed DIR+DSG method was set to 2, based on directional preference of the unsuppressed blood. In other words, the orientation of the diffusion vector was tilted toward the imaging plane.

Figure 3 demonstrates the tradeoff between vessel wall and luminal SNR as a function of *b*-value from a single volunteer. For a small *b*-value (<0.01 seconds/mm^2) the vessel wall signal experienced moderate attenuation consistent with T_2 decay but significant residual blood signal persisted, presumably due to slow or cyclical flow. As the *b*-value increased beyond 1 second/mm^2, the residual blood signal approached the noise floor but the vessel wall signal was also severely attenuated, presumably due to sensitivity to eddy current and diffusion effects. The *b*-value of 0.1 second/mm^2 appeared to be a reasonable compromise between blood suppression and maintenance of
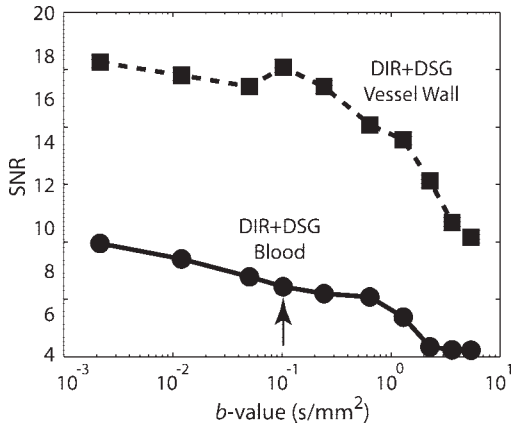
Figure 3. Blood and vessel wall SNR from a single volunteer, when using 3D IV-FSE DIR+DSG imaging with a range of *b*-values. Blood signal (solid) decreases with higher *b*-value. Vessel wall signal (dashed) decreases significantly for *b*-value > 1 second/mm^2. This is due to increased DSG duration and therefore significant T_2-weighting. A *b*-value of 0.1 second/mm^2 was used in subsequent studies (black arrow).

high contrast between vessel wall and lumen, and was used in the remaining studies. Note that a three-fold increase from the suggested *b*-value of 0.1 sec-

ond/mm^2 carries a less than 10% penalty in contrast between wall and lumen.

In Vivo Comparison

Figure 4 contains representative images from one volunteer at multiple axial locations acquired using all three methods. Images acquired using the 3D IV-FSE DIR method suffer from significant artifacts related to inadequate blood suppression in the carotid lumen. The images acquired using 2D multislice FSE DIR and 3D IV-FSE DIR+DSG exhibit comparable blood suppression across all the slices. Figure 5 shows the critical central slice near the carotid bifurcation from all five volunteers. This slice has the highest likelihood of residual blood signal. Unsuppressed blood signal is visible in images acquired from three of the five subjects using the 3D IV-FSE DIR method while the images acquired using the 2D FSE and 3D IV-FSE DIR+DSG methods remain relatively artifact free.

Figure 6a shows scatter plots of the measured SNRs and CNR$_{eff}$ from one central slice in each subject that contained the bifurcation. Luminal SNR using the proposed method was significantly lower than 3D IV-FSE DIR. Vessel wall SNR using the proposed method
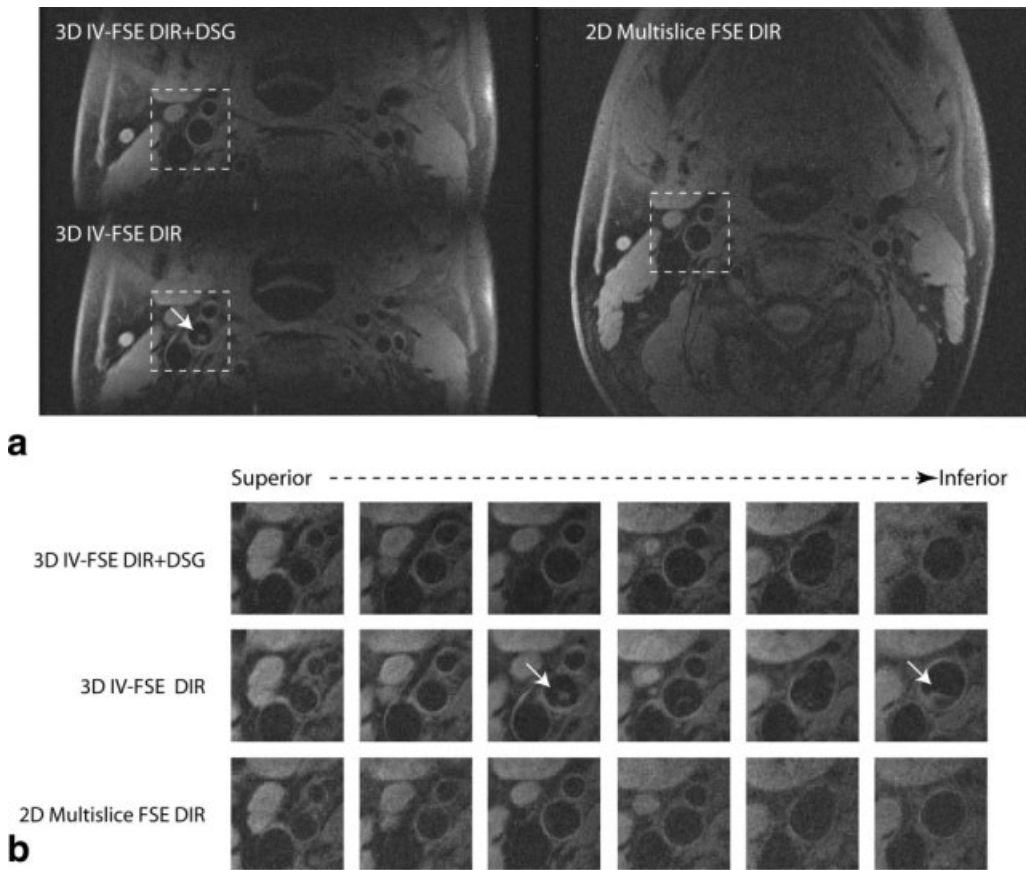
Figure 4. T_1-weighted images from a healthy volunteer at the bifurcation of carotid artery using the proposed 3D IV-FSE DIR+DSG, 3D IV-FSE DIR, and 2D multislice FSE DIR acquisitions. **a:** Full FOV single slice just above the bifurcation. The DIR only methods suffer from artifacts due to incomplete blood suppression at the bifurcation (arrow). **b:** Zoomed in view from all the slices around the right carotid artery, highlighted box indicates the slices with significant residual blood signal when using DIR alone. The arrow clearly indicates the presence of significant residual luminal blood signal when using 3D IV-FSE DIR.

Figure 5. T_1-weighted images from five volunteers at the bifurcation of the left carotid artery using the proposed 3D IV-FSE DIR+DSG, 3D IV-FSE DIR, and 2D multislice FSE DIR acquisitions. The highlighted box indicates studies with significant residual blood signal when using DIR alone. The arrows clearly indicate the presence of significant residual luminal blood signal when using 3D IV-FSE DIR.
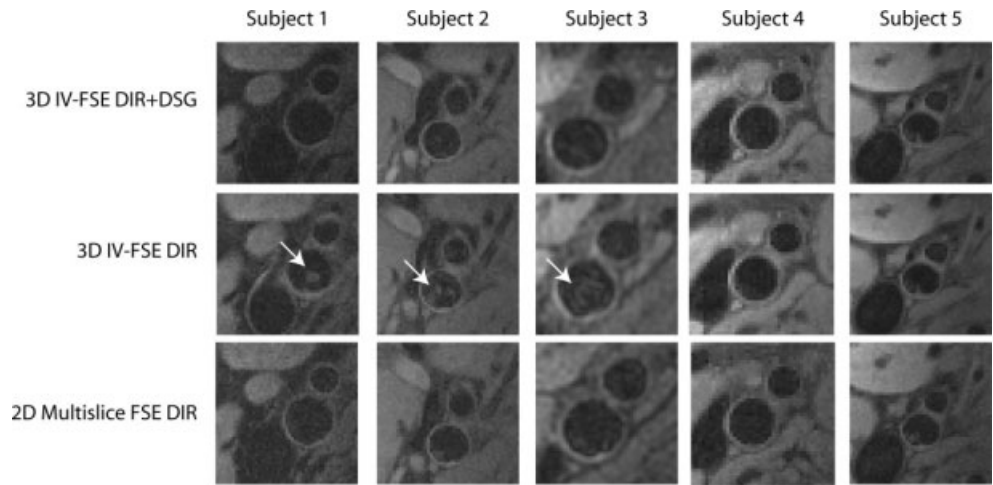
was comparable to 3D IV-FSE DIR. Vessel wall to lumen CNR$_{eff}$ using proposed method was statistically better than both 2D multislice FSE DIR and 3D IV-FSE DIR. Since sequence timing was same for the two 3D methods, the improvement in CNR is identical to the improvement in CNR$_{eff}$ when comparing the proposed method to 3D IV-FSE DIR. Table 1 summarizes the corresponding *P*-value comparisons across all three methods for the central slices that contain the bifurcation. The lumen SNR and wall to lumen CNR$_{eff}$ for the proposed 3D IV-FSE DIR+DSG technique were both statistically different from 3D IV-FSE DIR with $P < 0.001$ (6.96 vs. 14.15 for lumen SNR and 20.25 vs. 15.12 for CNR$_{eff}$). The wall SNR for the proposed

method was not statistically different from 3D IV-FSE DIR with $P = 0.26$ (28.9 vs. 29.8). Figure 6b shows a scatter plot of the measured SNRs and CNR$_{eff}$ averaged across all slices per subject, demonstrating similar trends.

DISCUSSION

DIR becomes a less effective method for blood suppression as the S/I thickness of the imaging slab increases. This is due to inadequate inflow of inverted blood spins into the imaging slab and diminished outflow of unaffected blood spins from the imaging slab.

Figure 6. Scatter plots showing in vivo measurements of the wall and lumen SNR, and wall to lumen CNR efficiency on a per subject basis. Each color represents one volunteer. **a:** Measurements from carotid segments only corresponding to the central slices at the bifurcation are plotted. **b:** Measurements from all carotid segments across all the acquired slices are averaged per subject and then plotted. The proposed method provides improved blood suppression and wall to lumen CNR$_{eff}$, for all subjects when compared to the 3D DIR IV-FSE.
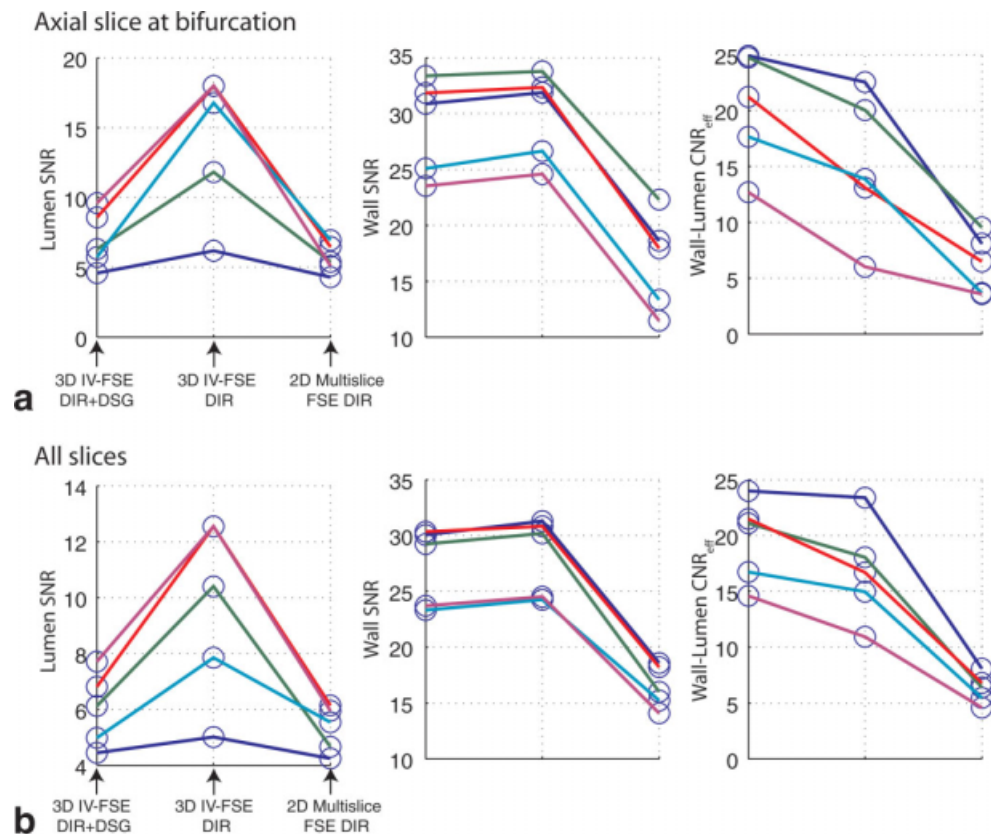
Table 1

P-Values for Paired *t*-Tests Comparing SNR and CNR$_{eff}$ of the Three Methods Based on all Subjects and Only Slices Containing the Carotid Bifurcation

	3D IV-FSE DIR+DSG vs. 3D IV-FSE DIR	3D IV-FSE DIR vs. 2D Multislice FSE DIR	3D IV-FSE DIR+DSG vs. 2D Multislice FSE DIR
SNR – lumen	<0.001	<0.001	0.06
SNR – wall	0.26	<0.001	<0.001
CNR$_{eff}$ – wall-lumen	<0.001	<0.001	<0.001

Subjects with stagnant flow are more likely to suffer from artifacts due to residual blood signal. In this study, significant residual blood signal was found in three of five subjects when data was acquired with the 3D IV-FSE DIR method. Here it is worthwhile to note that healthy volunteers are more likely to have stagnant flow than patients with stenosis. The proposed 3D IV-FSE DIR+DSG method produced complete blood suppression, comparable to that of the 2D multislice technique.

The typical implementation of DSG preparation involves applying gradients on all three axes with equal gradient strength (18,20). This is essentially done to maximally dephase the flowing spins but without accounting for the directional preference of flow. In the proposed DIR+DSG implementation, DIR preparation suppresses most of the flowing spins that have a directional preference along the carotid axis or orthogonal to the imaging slab. Blood spins that do not flow out of the imaging slab have a directional preference orthogonal to the vessel axis and may be suppressed by aligning the diffusion vector toward the imaging slab. Hence the area of the diffusion gradients aligned with the imaging slab is set higher than component perpendicular to the imaging slab.

The proposed DIR+DSG preparation inherits some drawbacks of the DSG alone preparation, including potential vessel wall signal loss due to true diffusion effect, T_2-weighting, and sensitivity to eddy current. However, these drawbacks are mitigated when using the proposed hybrid preparation due to shortened duration of the DSG module and the smaller *b*-value of flow dephasing bipolar gradients. This is evidenced by the fact that there was no significant difference in vessel wall SNR when comparing DIR+DSG with DIR alone.

There has been some debate on how to parameterize the blood suppression capability of DSG preparation. In Ref. 19, *b*-value was used for quantifying various amounts of sensitization, while in Ref. 20 the gradient first moment was used. This is because suppression may result from flow-induced phase rather than an actual diffusion effect. Here, we prefer the *b*-value parameterization since the hemodynamics at the carotid bifurcation are relatively complex and the blood spins within a voxel may have a distribution of accelerations in addition to a distribution of velocities. There is no clear evidence to date that indicates that the phase dispersion is resulting only from the gradient first moment and not the higher moments.

The proposed 3D IV-FSE DIR+DSG scheme achieved comparable image quality with respect to the various protocols but with a 40% reduction from the conventional 2D multislice FSE DIR scan time. The expected SNR improvement with the 3D techniques compared to the 2D technique is approximately 78% but the measured gain in SNR was approximately 68%. This is presumably due to the poor slice profile of the refocusing pulses, which causes a slight loss of signal in slices further from the slab center.

Mani et al (25) reported that gating did not affect image quality in black-blood multislice studies. However, in our experience the repeatability of ungated 3D IV-FSE is poor. We speculate that this was due to cumulative effect of vessel wall pulsation during the 3D scan which is of the order of 0.4 mm (26) and is comparable with the in-plane resolution used in our study. Also, this study was performed in healthy volunteers that are more likely to have compliant carotid vessel walls. Images obtained during this study were free of artifact related to swallowing or motion, presumably due to the short scan times. In patients unable to avoid swallowing, even during short scans, swallowing navigators may be necessary.

In conclusion, 3D IV-FSE acquisitions were combined with both DIR and DSG preparations for blood suppression, which proved to be more effective than DIR alone. Data acquired after the proposed hybrid DIR+DSG preparation was devoid of significant blood signal and blood-related artifacts. The reconstructed image quality was comparable to that of conventional 2D multislice FSE DIR method and vessel wall to lumen CNR$_{eff}$ was better than all competing methods. Furthermore, we demonstrate an 80-second acquisition of 3D carotid vessel wall data with $0.5 \times 0.5 \times 2.5$ mm^3 resolution, and a vessel wall to lumen CNR ≥ 20 throughout the bifurcation. This approach can be applied to proton-density, T_1-, and T_2-weighted FSE vessel wall imaging for accurate multispectral plaque quantitation within a reasonable examination time.

REFERENCES

1. Toussaint JF, LaMuraglia GM, Southern JF, Fuster V, Kantor HL. Magnetic resonance images lipid, fibrous, calcified, hemorrhagic, and thrombotic components of human atherosclerosis in vivo. Circulation 1996;94:932–938.
2. Soila K, Nummi P, Ekfors T, Viamonte M, Kormano M. Proton relaxation times in arterial wall and atheromatous lesions in man. Invest Radiol 1986;21:411–415.
3. Shinnar M, Fallon JT, Wehrli S, et al. The diagnostic accuracy of ex vivo MRI for human atherosclerotic plaque characterization. Arterioscler Thromb Vasc Biol 1999;19:2756–2761.
4. Yuan C, Mitsumori LM, Ferguson MS, et al. In vivo accuracy of multispectral magnetic resonance imaging for identifying lipid-rich necrotic cores and intraplaque hemorrhage in advanced human carotid plaques. Circulation 2001;104:2051–2056.

5. Koktzoglou I, Chung Y, Mani V, et al. Multislice dark-blood carotid artery wall imaging: a 1.5 T and 3.0 T comparison. J Magn Reson Imaging 2006;23:699–705.

6. Yarnykh VL, Terashima M, Hayes CE, et al. Multicontrast black-blood MRI of carotid arteries: comparison between 1.5 and 3 Tesla magnetic field strengths. J Magn Reson Imaging 2006;23:691–698.

7. Kim SE, Kholmovski EG, Jeong EK, Buswell HR, Tsuruda JS, Parker DL. Triple contrast technique for black blood imaging with double inversion preparation. Magn Reson Med 2004;52:1379–1387.

8. Mani V, Itskovich VV, Szimtenings M, et al. Rapid extended coverage simultaneous multisection black-blood vessel wall MR imaging. Radiology 2004;232:281–288.

9. Song HK, Wright AC, Wolf RL, Wehrli FW. Multislice double inversion pulse sequence for efficient black-blood MRI. Magn Reson Med 2002;47:616–620.

10. Yarnykh VL, Yuan C. Multislice double inversion-recovery black-blood imaging with simultaneous slice reinversion. J Magn Reson Imaging 2003;17:478–483.

11. Itskovich VV, Mani V, Mizsei G, et al. Parallel and nonparallel simultaneous multislice black-blood double inversion recovery techniques for vessel wall imaging. J Magn Reson Imaging 2004;19:459–467.

12. Hardy CJ, Dixon WT, Blezek DJ, Saranathan M, Zong X, Raman SV. Increased slice coverage for black blood arterial wall imaging with double-inversion FSE. In: Proceedings of the 12th Annual Meeting of ISMRM, Kyoto, Japan, 2004 (Abstract 450).

13. Crowe LA, Gatehouse P, Yang GZ, et al. Volume-selective 3D turbo spin echo imaging for vascular wall imaging and distensibility measurement. J Magn Reson Imaging 2003;17:572–580.

14. Conturo TE, Price RR, Beth AH. Rapid local rectangular views and magnifications: reduced phase encoding of orthogonally excited spin echoes. Magn Reson Med 1988;6:418–429.

15. Mitsouras D, Mulkern RV, Rybicki FJ. Strategies for inner volume 3D fast spin echo magnetic resonance imaging using non-selective refocusing radio frequency pulses. Med Phys 2006;33:173–186.

16. Crowe LA, Varghese A, Mohiaddin RH, Yang GZ, Firmin DN. Elimination of residual blood flow-related signal in 3D volume-selective TSE arterial wall imaging using velocity-sensitive phase reconstruction. J Magn Reson Imaging 2006;23:416–421.

17. Steinman DA, Rutt BK. On the nature and reduction of plaque-mimicking flow artifacts in black blood MRI of the carotid bifurcation. Magn Reson Med 1998;39:635–641.

18. Sirol M, Itskovich VV, Mani V, et al. Lipid-rich atherosclerotic plaques detected by gadofluorine-enhanced in vivo magnetic resonance imaging. Circulation 2004;109:2890–2896.

19. Koktzoglou I, Li D. Diffusion-prepared segmented steady-state free precession: Application to 3D black-blood cardiovascular magnetic resonance of the thoracic aorta and carotid artery walls. J Cardiovasc Magn Reson 2007;9:33–42.

20. Wang J, Yarnykh VL, Hatsukami T, Chu B, Balu N, Yuan C. Improved suppression of plaque-mimicking artifacts in black-blood carotid atherosclerosis imaging using a multislice motion-sensitized driven equilibrium (MSDE) turbo spin-echo (TSE) sequence. Magn Reson Med 2007;58:973–981.

21. Edelman RR, Chien D, Kim D. Fast selective black blood MR imaging. Radiology 1991;181:655–660.

22. Lu H, Fuster V, Clingman C, Golay X, VanZijl PCM. Determining the longitudinal relaxation time (T_1) of blood at 3.0 Tesla. Circulation 2000;102:506–510.

23. Fayad ZA, Fuster V, Fallon JT, et al. Noninvasive in vivo human coronary artery lumen and wall imaging using black-blood magnetic resonance imaging. Circulation 2000;102:506–510.

24. Brittain JH, Hu BS, Wright GA, Meyer CH, Macovski A, Nishimura DG. Coronary angiography with magnetization-prepared T_2 contrast. Magn Reson Med 1995;33:689–696.

25. Mani V, Itskovich VV, Aguiar SH, et al. Comparison of gated and non-gated fast multislice black-blood carotid imaging using rapid extended coverage and inflow/outflow saturation techniques. J Magn Reson Imaging 2005;22:628–633.

26. Selzer RH, Mack WJ, Lee PL, Fu HK, Hodis HN. Improved common carotid elasticity and intima-media thickness measurements from computer analysis of sequential ultrasound frames. Atherosclerosis 2001;154:185–193.